

M odulated A m plitude W aves in C ollisionally Inhom ogeneous B ose-E instein C ondensates

M aison A . Porter

D epartment of P hysics and C enter for the P hysics of I nformation,
C alifornia I nstitute of T echnology, P asadena, CA 91125, U SA

P . G . K evrekidis

D epartment of M athematics and S tatistics,
U niversity of M assachusetts, A mherst M A 01003, U SA

B oris A . M alomed

D epartment of I nterdisciplinary S tudies,
S chool of E lectrical E ngineering, F aculty of E ngineering,
T el A viv U niversity, T el A viv 69978, I srael

D . J . F rantzeskakis

D epartment of P hysics, U niversity of A thens,
P anepistim iopolis, Z ografos, A thens 15784, G reece

Abstract

We investigate the dynamics of an effectively one-dimensional Bose-Einstein condensate (BEC) with the scattering length a subjected to a spatially periodic modulation, $a = a(x) = a(x + L)$. This "collisionally inhomogeneous" BEC is described by a Gross-Pitaevskii (GP) equation with a nonlinearity coefficient that is a periodic function of x . We transform this GP equation into a constant-nonlinearity GP equation with an effective potential and study a class of the latter's extended wave solutions. For small inhomogeneities, the effective potential takes a form reminiscent of a superlattice, and the amplitude dynamics of the BEC's coherent structures are described by a nonlinear generalized Ince equation. In the small-amplitude limit, we use averaging to construct modulated amplitude wave (MAW) solutions, whose stability we subsequently examine using both numerical simulations of the original GP equation and fixed point computations with the MAW as numerically exact solutions. We show that "on-site" solutions, whose maxima correspond to maxima of the "nonlinear lattice" $a(x)$, are significantly more stable than "off-site" solutions.

Keywords: Bose-Einstein condensates, periodic potentials, multiple-scale perturbation theory, Hamiltonian systems

I. INTRODUCTION

Among the most prominent differential equations in applied mathematics are nonlinear Schrödinger equations, a class of partial differential equations which have been employed as models in diverse branches of physics [1]. Such work has come to the forefront in recent years because of the enormous theoretical and experimental progress that has occurred in the study of atomic Bose-Einstein condensates (BECs) [2] and nonlinear optics [3]. As there is a formal similarity between coherent matterwaves and photons, these disciplines are closely connected and continuously impact each other. This is very important not only from a theoretical perspective but also for applications. For example, coherent matterwaves can be manipulated utilizing relevant devices, such as atom chips [4], and thus can potentially be used in future applications reminiscent of their optical counterparts.

In the mean-field approximation, and at sufficiently low temperatures, matterwaves are accurately modeled by a cubic nonlinear Schrödinger equation (NLS) incorporating an external potential. In this context, the NLS equation is also known as the Gross-Pitaevskii (GP) equation [2]:

$$i\hbar \frac{\partial \psi}{\partial t} = -\frac{\hbar^2}{2m} \nabla^2 \psi + g|\psi|^2 \psi + V(\mathbf{r}) \quad ; \quad (1)$$

where \hbar is the Planck's constant, $\psi(\mathbf{r}; t)$ is the macroscopic wave function of the condensate, normalized to the number of atoms N (so that $\int_{\mathbb{R}^3} |\psi|^2 d\mathbf{r} = N$), $V(\mathbf{r})$ is the external potential, and the effective interaction constant is $g = (4\pi \hbar^2 a m) [1 + O(\frac{1}{N})]$, where a is the s-wave scattering length, m is the atomic mass, and $\int_{\mathbb{R}^3} |\psi|^4 d\mathbf{r}$ is a measure of the density [2].

The properties of BECs, including their shape, collective excitations, statistical fluctuations, and the dynamics of their nonlinear excitations (such as solitons and vortices), are determined by the sign and magnitude of the scattering length a . Accordingly, one of the key tools used in current studies of BECs relies on adjusting a (and hence the nonlinearity coefficient g defined above). A well-known way to achieve this goal is to tune an external magnetic field in the vicinity of a Feshbach resonance [5, 6, 7]. Alternatively, one can use

the Feshbach resonance induced by an optical [8] or dc electric [9] field. In low-dimensional settings, one can also tune the effective scattering length by changing the BEC's transversal component [10].

Varying the BEC scattering length globally (i.e., temporally modulating a) has been crucial to many important experimental discoveries, including the formation of molecular condensates [11] and probing the so-called BEC-BCS crossover [12]. Additionally, recent theoretical studies have predicted that a time-dependent modulation of the scattering length can be used to stabilize attractive condensates in two [13] and three [14] dimensions [in the latter case, the Feshbach resonance-based technique should be combined with a quasi-one-dimensional (quasi-1D) periodic potential, known as an optical lattice (OL)] and to create robust after-wave solitons [15].

On the other hand, the possibility of varying the scattering length locally (i.e., spatially) has also recently been proposed [16, 17, 18, 19]. Such spatial dependence of the scattering length, which can be implemented by utilizing a spatially inhomogeneous external magnetic field in the vicinity of a Feshbach resonance [17, 18], renders the collisional dynamics inhomogeneous across the BEC. These so-called "collisionally inhomogeneous" BECs have recently attracted considerable attention, as they are relevant to many interesting studies and applications, including adiabatic compression of after-waves [16, 18], Bloch oscillations of after-wave solitons [18], atom lasers [19, 20], enhancement of transmittivity of after-waves through barriers [21, 22], and the dynamics of after-waves in the presence of periodic or random spatial variations of the scattering length [23]. Note that while the above works chiefly concentrated on quasi-1D condensates, relevant studies in a quasi-two-dimensional (quasi-2D) setting were also recently reported [24] (see also Ref. [25] for a qualitatively similar model in a different physical context).

In the present work, we consider an effectively one-dimensional BEC with a scattering length subjected to a periodic variation, so that $a(x) = a(x + L)$ for some period L . This configuration, with such a nonlinear lattice, can be realized experimentally (see, e.g., the diagram in Ref. [20]) and it offers various possibilities for the study of after-wave solitons (as discussed in, e.g., Refs. [23, 24, 26]). Here, however, we focus on the dynamics of spatially extended states (rather than solitons), which has not yet been considered in earlier works. Extended states can be created experimentally, as has been done previously, for example, in the optical superlattice setting [27].

The analysis of the problem under consideration, as well as the organization of the paper, proceeds as follows. First, we apply a transformation to the quasi-1D GP equation with the nonlinearity coefficient periodically modulated in space in order to derive an effective GP equation with a constant nonlinearity coefficient. With this transformation, the original inhomogeneity is mapped into an effective linear (superlattice) potential term. We then consider spatially extended solutions of the effective GP equation in the form of modulated amplitude waves (M AWs), whose slow-amplitude dynamics we derive using an averaging method. These analytical considerations (in section II) are followed by an investigation of the dynamics and stability of the M AWs in section III, using both direct numerical simulations of the original GP equation and fixed-point computations with the M AWs as numerically exact solutions. We thereby show that "on-site" solutions, whose maxima correspond to maxima of the nonlinear lattice, tend to be more stable than "off-site" solutions. We summarize our findings and present our conclusions in section IV. Some technical details of the averaging procedure are then discussed in an appendix (section V).

II. THE PERTURBED GROSS-PITAEVSKII EQUATION

The 3D GP equation (1) can be reduced to an effectively 1D form, provided that the transverse dimensions of the BEC are on the order of its healing length and its longitudinal dimension is much larger than the transverse ones [28]. In this regime, the 1D approximation is derived by averaging Eq. (1) in the transverse plane. One can readily show (see, e.g., Ref. [18]) that the resulting 1D GP equation takes the following dimensionless form:

$$iu_t = \frac{1}{2}u_{xx} + g(x)ju_j^2u + V(x)u; \quad (2)$$

where we recall that nonlinearity coefficient $g(x)$ varies in space. In Eq. (2), u is the mean-field wavefunction (with the density ju_j^2 measured in units of the peak 1D density n_0), x and t are normalized, respectively, to the healing length $\lambda = \sqrt{\frac{p}{n_0 g_0 j m}}$ and c (where $c = \sqrt{\frac{p}{n_0 g_0 j m}}$ is the Bogoliubov speed of sound), and energy is measured in units of the chemical potential $\mu = g_0 n_0$. In the above expressions, $g_0 = 2\pi!_z a(B_0)$, where $!_z$ denotes the confining frequency in the transverse direction. Finally, $V(x)$ is the rescaled external trapping potential, and the x -dependent nonlinearity is given by $g(x) = a(x)/a(B_0)$, where $a(x)$ is the spatially varying scattering length and B_0 is a characteristic value of the external

magnetic field (that is relatively close to the Feshbach resonance).

We will examine periodic modulations of the scattering length, considering a spatially varying nonlinearity of the form

$$g(x) = g_0 + V_0 \sin^2(x); \quad (3)$$

where V_0 and g_0 are, respectively, the amplitude and wavenumber of the modulation. Such a spatial periodicity can be induced experimentally by applying a periodically patterned configuration of the external magnetic/optical/electric field that controls the Feshbach resonance. We shall focus on the case of repulsive BECs and thus let $g_0 > 0$; we also assume that $V_0 > 0$. For attractive BECs, for which $g_0 < 0$, one can also transform the nonlinear equation (2) into an effective GP equation with a constant nonlinearity coefficient (see below).

We now introduce the transformation $v = \frac{p}{g(x)}u$, which casts Eq. (2) in the form

$$\begin{aligned} i\dot{v}_t &= \frac{1}{2}v_{xx} + i\gamma' v + V(x)v + \hat{V}_e(x)v; \\ \hat{V}_e(x) &= \frac{1}{2}f^{(0)} - \frac{f^{(0)2}}{f^2} + \frac{f^{(0)}@}{f@x}; \end{aligned} \quad (4)$$

where $f(x) = \sqrt{g(x)}$, and the prime stands for d/dx in the effective potential operator $\hat{V}_e(x)$.

If the scattering length modulation is weak [i.e., $V_0 \ll g_0$ in Eq. (3)], then \hat{V}_e can be considered as a superlattice potential (because it contains a second harmonic in addition to the fundamental one) plus a first-derivative operator term:

$$\hat{V}_e(x) = \frac{3^2 V_0^2}{16g_0^2} + \frac{2V_0}{2g_0} \cos(2x) + \frac{3^2 V_0^2}{16g_0^2} \cos(4x) + \frac{V_0}{2g_0} \sin(2x) \frac{@}{@x}; \quad (5)$$

Because $V_0 \ll g_0$, we can define the small parameter " $V_0=g_0$ ", evincing the fact that the $\cos(4x)$ harmonic in Eq. (5) is a small correction to the fundamental harmonic, $\cos(2x)$. That is, to $O(1)$, the effective potential (5) is a modified lattice rather than a superlattice.

III. MODULATED AMPLITUDE WAVES

We consider solutions to Eqs. (4,5) that describe coherent structures of the form

$$v(x;t) = R(x) \exp(i[\phi(x) - Et]) : \quad (6)$$

When temporally periodic waves given by this expression are also spatially periodic, they are called modulated amplitude waves (MAWs). Such nonlinear waves have been studied previously in BEC models with optical-lattice and superlattice potentials [29, 30, 31, 32].

Inserting Eq. (6) in Eq. (4) and equating the real and imaginary components of the resulting equation yields an ordinary differential equation governing the spatial amplitude dynamics. For standing waves (for which $\langle x \rangle = 0$), this equation is

$$\frac{d^2 R}{dx^2} - \frac{dR}{dx} \sin(2x) + 2\tilde{\omega}'' \cos(2x) - \frac{3}{8}\tilde{w}^2 \cos(4x) - 2V(x)R - 2R^3 = 0; \quad (7)$$

where $2\tilde{\omega} = 2\omega + (3\tilde{w}^2)^{1/2}$. Equation (7), known as a nonlinear generalized Ince equation [33], is reminiscent of the nonlinear Mathieu equation, but with the parametric force acting on both R and R^0 .

A. Small-Amplitude Solutions

Let us now consider Eq. (7) in the absence of the external trapping potential $V(x)$. As shown by Eqs. (4) and (5), the effective superlattice potential $\hat{V}_e(x)$ is already a confining potential for the condensate. Seeking small-amplitude solutions, we employ the scaling $R^0 \xrightarrow{p} \tilde{w} = 2s$, which transforms Eq. (7) into

$$\frac{d^2 s}{dx^2} - \tilde{w} \sin(2x) \frac{ds}{dx} + \tilde{\omega}^2 - \tilde{w} \cos(2x) - \frac{3}{8}\tilde{w}^2 \cos(4x) s - \tilde{w}^3 = 0; \quad (8)$$

where $\tilde{\omega}^2 = 2\tilde{\omega}^2$ (implying that $\tilde{\omega}$ is positive). The alternative scaling $R^0 \xrightarrow{p} \tilde{w} = \frac{1}{2}$ would produce a nonlinearity of size $O(\tilde{w}^2)$ rather than $O(\tilde{w}^4)$ in Eq. (8) and would lead one even deeper into the small-amplitude regime.

Equation (8) is of the form

$$s^{(0)} + \tilde{\omega}^2 s = \tilde{w} F_1(s; s^0; x) + \tilde{w}^2 F_2(s; s^0; x); \quad (9)$$

where

$$\begin{aligned} F_1(s; s^0; x) &= s \cos(2x) + \frac{3}{8} s \sin(2x) + s^3; \\ F_2(s; s^0; x) &= \frac{3s}{8} \cos(4x); \end{aligned} \quad (10)$$

As in Ref. [32], we consider situations near the 2:1 subharmonic resonance, for which $\tilde{\omega} = \tilde{w}$ in Eq. (9). Assuming a small 'detuning' from the exact resonance, we introduce the

expansion

$$= + " \cdot 1 + " \cdot 2 + O ("^3); \quad (11)$$

which we insert in Eq. (9) to obtain

$$s^0 + " \cdot 2 s = " G_1(s; s^0; x) + " \cdot 2 G_2(s; s^0; x) + O ("^3); \quad (12)$$

where

$$\begin{aligned} G_1(s; s^0; x) &= 2_1 s + F_1(s; s^0; x); \\ G_2(s; s^0; x) &= 2_1^2 + 2_2 s + F_2(s; s^0; x); \end{aligned} \quad (13)$$

When $" = 0$, Eq. (12) has the solution

$$s = \cos(x + \phi); \quad (14)$$

with first derivative $s^0 = -\sin(x + \phi)$. We now use the solution (14) and its derivative as a starting point to apply the method of variation of parameters to equation (12). We therefore seek a solution to Eq. (12) in the form

$$s(x) = \phi(x) \cos(x + \phi(x)); \quad s'(x) = \phi'(x) \sin(x + \phi(x)); \quad (15)$$

where $\phi(x)$ and $\phi'(x)$ are slowly varying functions. Differentiating the expression for $s(x)$ in Eq. (15), we enforce the following consistency condition with the expression for $s^0(x)$ in (15):

$$^0 \cos(x + \phi) = -^0 \sin(x + \phi); \quad (16)$$

Then, inserting the result in Eq. (12) yields

$$\begin{aligned} ^0 &= -\sin(x + \phi) G_1(\cos(x + \phi); \sin(x + \phi); x) \\ &\quad -\sin(x + \phi) G_2(\cos(x + \phi); \sin(x + \phi); x); \end{aligned} \quad (17)$$

$$\begin{aligned} ^0 &= -\cos(x + \phi) G_1(\cos(x + \phi); \sin(x + \phi); x) \\ &\quad -\cos(x + \phi) G_2(\cos(x + \phi); \sin(x + \phi); x); \end{aligned} \quad (18)$$

Our objective is to isolate the components of $\phi(x)$ and $\phi'(x)$ that vary slowly as compared to the fast oscillations of $\cos(x)$ and $\sin(x)$ and to derive averaged equations governing

the dynamics of these parts. To commence averaging, we decompose c and ϵ into a sum of the slowly varying parts and small, rapidly oscillating corrections. That is,

$$\begin{aligned} &= c + "w_1(c; \epsilon; x) + "^2 v_1(c; \epsilon; x) + O("^3); \\ &= \epsilon + "w_2(c; \epsilon; x) + "^2 v_2(c; \epsilon; x) + O("^3); \end{aligned} \quad (19)$$

We then substitute Eqs. (19) into Eqs. (17)–(18) and Taylor-expand to obtain

$$\begin{aligned} c^0 &= " \frac{\partial w_1}{\partial x} - \frac{1}{c} \sin(x + \epsilon) G_1(c \cos(x + \epsilon); c \sin(x + \epsilon); x) \\ &+ "^2 \frac{\partial v_1}{\partial x} + L_1(c; \epsilon; x) + O("^3); \end{aligned} \quad (20)$$

$$\begin{aligned} \epsilon^0 &= " \frac{\partial w_2}{\partial x} - \frac{1}{c} \cos(x + \epsilon) G_1(c \cos(x + \epsilon); c \sin(x + \epsilon); x) \\ &+ "^2 \frac{\partial v_2}{\partial x} + L_2(c; \epsilon; x) + O("^3); \end{aligned} \quad (21)$$

The functions w_1 and w_2 in Eqs. (19)–(21) should be chosen so as to eliminate all the rapidly oscillating terms at order $O(")$. At $O("^2)$, the functions v_1 and v_2 are similarly chosen. The terms $L_1(c; \epsilon; x)$ and $L_2(c; \epsilon; x)$ in Eqs. (20)–(21) depend on w_1 , w_2 , G_1 , and G_2 . We provide expressions for w_1 , w_2 and L_1 , L_2 in the Appendix. (Note that expressions for $v_1(x)$ and $v_2(x)$ are not needed until one tackles the third-order corrections, so we do not display them.) The functions G_1 and G_2 are expressed in terms of c and ϵ as follows:

$$\begin{aligned} G_1(c; \epsilon; x) &= 2_1 c \cos(x + \epsilon) + c \cos(x + \epsilon) \cos(2x) - c \sin(x + \epsilon) \sin(2x) + 3 \cos^3(x + \epsilon); \\ G_2(c; \epsilon; x) &= 2_2 c \cos(x + \epsilon) + \frac{3}{8} c \cos(x + \epsilon) \cos(4x); \end{aligned}$$

To first order, the slow evolution equations are

$$c^0 = O("^2); \quad \epsilon^0 = " \frac{3c^2}{8} + O("^2); \quad (22)$$

generating a circle of nonzero equilibria with amplitude $c = \sqrt[3]{\frac{8}{3}} = 3$. The generating functions $w_1(x)$ and $w_2(x)$ that yield these equations are shown in the Appendix. This process results in the amplitude function

$$R(x) = \frac{c}{2} \cos(x + \epsilon) - v(x; t=0); \quad (23)$$

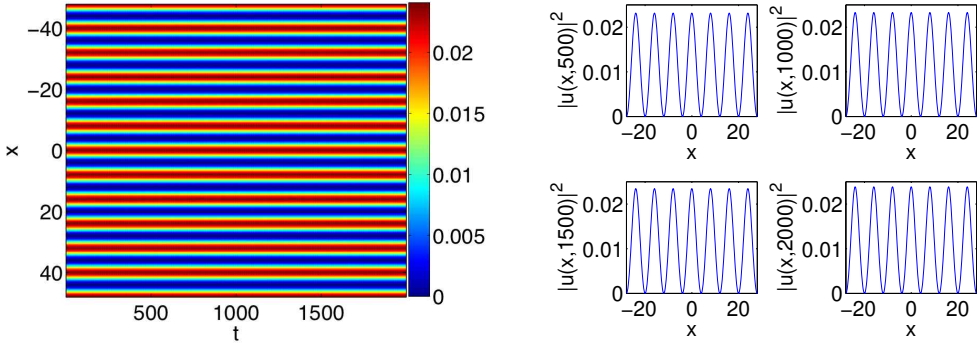


FIG. 1: (Color online) Dynamical evolution of the sinusoidal M AW of Eq. (23) with parameter values $\gamma = 0$ for $g_0 = 2$, $\omega = 8$, $V_0 = 0.15$, $\omega_1 = 3$, and $\omega_2 = 1$. The left panel shows the space-time contour plot of the square modulus (density) $|u|^2$ of the solution, and the right panels show four snapshots (spatial profiles) of the spatio-temporal evolution. The dynamics illustrate an apparent stability of the solution up through at least $t = 2000$.

where the phase shift ϕ is arbitrary. The corresponding M AW is given by $v(x,t) = R(x) \exp(-i\phi)$, as per Eq. 6).

Returning to the original GP equation (in the absence of an external potential), we obtain the M AW $u(x,t) = v(x,t) = \frac{R(x,t)}{g(x,t)}$. We examine its dynamics and stability with direct simulations of Eq. (2) with $V(x) = 0$. Results of the simulations for $g_0 = 2$, $V_0 = 0.15$, $\omega = 8$ (so that $\omega_0 = 0.0295$), $\omega_1 = 3$, $\omega_2 = 1$, and $\phi = 0$ are shown in Fig. 1. Note that these parameter values correspond to a ^{87}Rb (or a ^{23}Na) condensate, in a trap with transverse confining frequency $\omega_0 = 2\pi \approx 1000\text{Hz}$, that contains $N = 10^8$ atoms with a peak 1D density $n_0 = 10^8 \text{ m}^{-1}$. Here, the spatial unit (i.e., the healing length) is $\lambda = 0.3 \text{ m}$ ($\omega_0 = 0.9 \text{ m}$), and the temporal unit is $\tau = c = 0.14 \text{ ms}$ ($\omega_0 = 0.3 \text{ ms}$). Figure 1 shows that the M AW appears to be stable for long times as a solution of the original GP equation. For larger ω , however, the wave breaks up into solitary packets (that appear to be localized around the maximum of the nonlinear optical lattice; see the discussion below), as indicated in Fig. 2 (for $V_0 = 1.5$). In fact, as we will discuss below, the apparently stable M AWs obtained for small V_0 are actually weakly unstable, although their lifetimes are long. The normalized time $t = 2000$ amounts to 280 ms for a Rubidium (or 600 ms for a Sodium) BEC in real time, suggesting that these M AWs can nevertheless be observed in experiments.

One can also incorporate the generating functions into the M AWs and examine the sta-

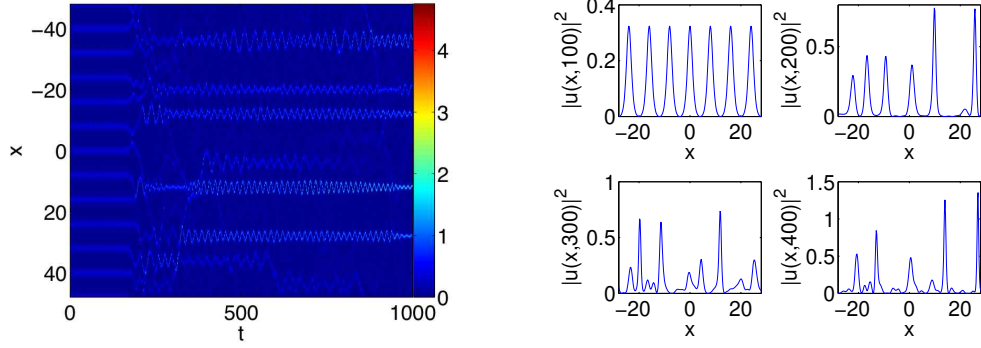


FIG. 2: (Color online) Same as Fig. 1, but for $V_0 = 1.5$. As early as $t = 200$, the MAW solution starts breaking up into solitary lamens that appear to be localized around the maxima of the nonlinear optical lattice (see the discussion in the text).

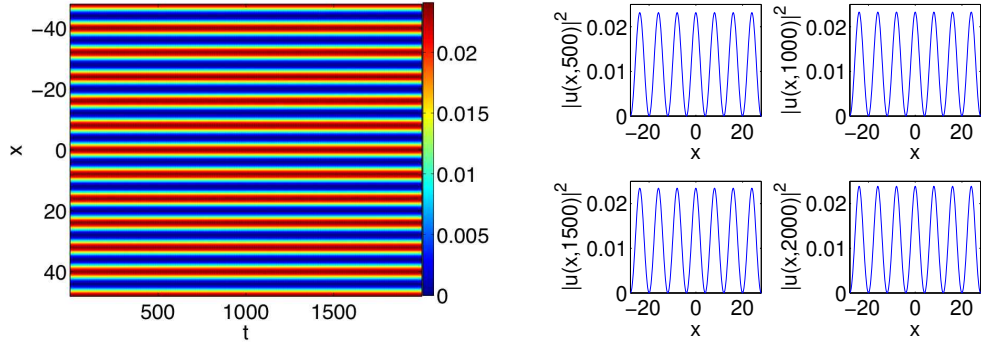


FIG. 3: (Color online) Same as Fig. 1 (and also with $V_0 = 0.15$), but for the refined prediction of the initial MAW solution based on Eq. (24). The solution also appears to be dynamically stable.

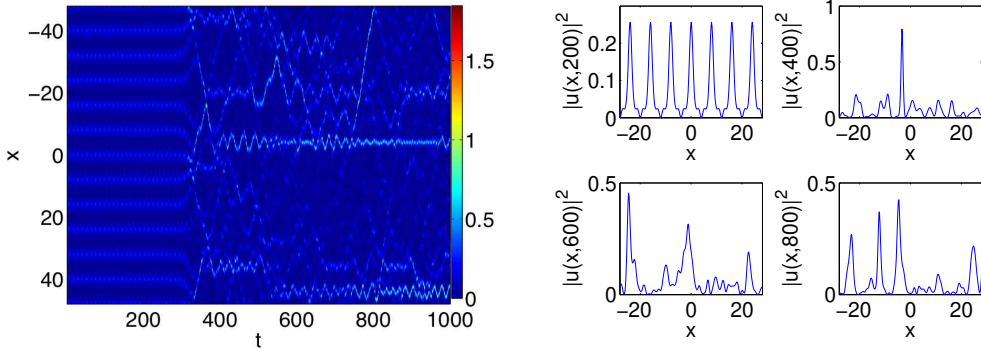


FIG. 4: (Color online) Same as Fig. 2, but with the MAW of Eq. (24) used as the initial condition for the time evolution of the GP equation. Observe that the refined initial condition leads to a delayed initiation of the instability (which now begins at about $t = 300$).

bility properties of the resulting refined M AWs using direct numerical simulations. These M AWs are given by

$$R(x) = \frac{r}{\pi} \left(c + "w_1 \right) \cos \left(x + ' + "w_2 \right) \quad v(x; t=0) \quad (24)$$

instead of Eq. (23). We plot the corresponding space-time plots and spatial profiles at various time instants for $V_0 = 0.15$ in Fig. 3 and for $V_0 = 1.5$ in Fig. 4. All other parameters are the same as before. It is readily observed that the instability in Fig. 4 sets in later (at $t = 300$) than that in Fig. 2 (at $t = 200$), which was obtained with the same parameter values using the sinusoidal M AW of Eq. (23).

The M AWs in Eqs. (23) and (24) were determined to order $O(")$, so they ignore the effects of the second-harmonic component of the lattice, which arise at $O("^2)$. To estimate the influence of this component, we used the same M AWs as initial conditions in direct simulations of the original GP equations in the presence of an additional external optical lattice (OL) potential, $V(x) = (3=16)^{1/2} \cos(4x)$ that exactly cancels out the second-harmonic component of the lattice. While differences between the results of the simulations with and without the compensating OL are not apparent in comparing space-time plots side-by-side, one can observe the slow development of small discrepancies by examining the time-evolution of the absolute value of their difference.

To second order, the equations of slow evolution are

$$\begin{aligned} c^0 &= "^2 \frac{c}{4} - 1 \frac{c^2}{8} \sin(2') + O("^3); \\ '^0 &= " - 1 \frac{3c^2}{8} + "^2 - 2 \frac{1}{16} + \frac{3c^2}{4^2} - 1 \frac{51c^4}{256^3} + \frac{1}{4} - 1 \frac{c^2}{4} \cos(2') + O("^3); \end{aligned} \quad (25)$$

In contrast to the first-order equations (22), the equilibrium points of Eqs. (25) depend on $"$, which is typical in second-order averaging. In studying the dynamics of slow-fast equations produced by such a procedure, one obtains, in general, a complicated bifurcation problem, which can be investigated by taking $"$ small but fixed (see, e.g., Ref. [34]). For our purposes, we simply note that the only difference between Eqs. (25) and the slow equations one would obtain at second order without the $O("^2)$ lattice term in Eq. (7) amounts to constant terms at the same order [they result directly from the detuning of ω ; see Eq. (11)]. Without the second-order lattice term, ω_2 would not be present, and there would be an additional

constant term, $\gamma_1^2 = (2)$, that is cancelled out here because of the extra harmonic. To study the effects of the second-order lattice system *attractively*, one can examine the dynamics starting with the alternative scaling $R^p \rightarrow \frac{p}{2}$ (rather than $R^p \rightarrow 2s$, as adopted above), in which case the effect of the nonlinearity also emerges at second order.

In the absence of resonances, second-order averaging yields slow dynamical equations for (c, \dot{c}) with $c^0 = 0$ ("³) and $\dot{c}^0 < 0$, so that a fixed-radius circle is traversed in the clockwise direction. From here, one can also consider resonances whose effects appear at $O(\epsilon^2)$.

B. Stability

In Figs. 2 and 4, we observe that the M AW initial conditions, derived for small V_0 , break down rather quickly for larger V_0 . In fact, there is a weak instability even for small V_0 , although the time it takes for the instability to set in is rather long (beyond $t = 2000$). Thus, the M AW solutions have a good chance to be observed experimentally (recall that $t = 2000$ corresponds to 280 ms for a ⁸⁷Rb BEC and 600 ms for a ²³Na one) for sufficiently small scattering length modulations V_0 .

To investigate this point further, we performed *fixed-point* computations using Eqs. (23) and (24) as starting guesses in order to obtain numerically exact stationary states. We show the results for Eq. (23) in Fig. 5 using a computational domain containing one period of the solution. In this context, we have implemented a variant of our finite-difference method (for the spatial discretization) that incorporates Floquet theory, as is described, e.g., in Section 4.3 of [35]. Adding an $\exp(i\omega)$ and its complex conjugate at the appropriate locations of our stability matrix, we fill in the bands of continuous spectrum by varying ω within the interval $[0; 2\pi]$. We used a partition of 200 equidistant points in ω for the results shown here. We find that the configuration is always unstable, even for the small V_0 that appeared to be stable based on direct numerical simulations. Hence, the apparent stability of Figs. 1 and 3 arises only because of the fact that the simulation was performed for a finite time (up to $t = 2000$). As indicated in Fig. 5 (where the spectral planes are also plotted in the bottom panels), the instability is weak for small V_0 but becomes strong for large V_0 .

To find more stable solutions, we note that the transformation $v^p \rightarrow g(x)u$ suggests with the nonlinear OL (unlike what is the case for linear OLs), solutions prefer to be centered on-site, so that their maxima coincide with maxima of the lattice rather than minima. This

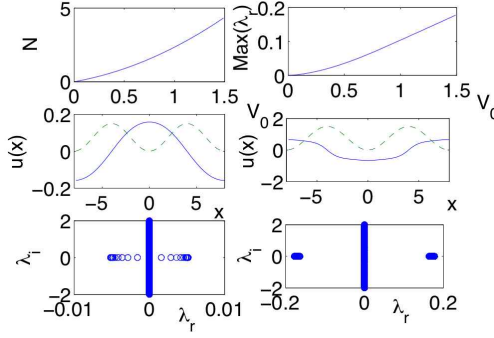


FIG. 5: (Color online) Results of a fixed point iteration to identify the solution given by Eq. (23) as a numerically exact stationary state. The top left panel shows the L^2 norm (density) of this state in our computational domain (containing one period of the solution), and the top right panel shows the maximal real part of the most unstable eigenvalue of the configuration. Observe that the configuration is always unstable. Hence, the apparent stability of Figs. 1 and 3 arises only because of the finite time (up to $t = 2000$) of the direct GP simulations. The middle left and right panels show the solution (solid curve) and nonlinear lattice $g(x)$ (dashed curve) for $V_0 = 0.15$ and $V_0 = 1.5$, respectively. The bottom left and right panels show the corresponding spectral planes of the solutions and indicate the weak instability of the former and the strong instability of the latter.

is not surprising, as the multiplicative terms (i.e., the ones without the $d=dx$) of $V_e(x)$ act as a regular (super)lattice after the transformation and the minima of $g(x)$ coincide with the maxima of these terms in $V_e(x)$. (We note in passing that this difference between linear and nonlinear OLS has also recently been highlighted in [36] from a spectral theory perspective for bright soliton solutions of the NLS equation.) We observe additionally in Figs. 2 and 4 that when the MAWs break up, one obtains solutions that are localized on maxima of the nonlinear OLS. We can take advantage of this observation by using MAWs with different phases' as initial wavefunctions in simulations of the GP equation (2).

We show the dynamical evolution of on-site MAWs (for which $\beta = -2$) in Figs. 6 and 7 for $V_0 = 0.15$ and $V_0 = 1.5$, respectively. As observed in Fig. 7, the solution remains stable past $t = 1000$ instead of breaking up far earlier, as was the case for off-site solutions. We confirm these observations on stability using fixed-point computations of the same type as above (but now for solutions with $\beta = -2$), the results of which are shown in Fig. 8. We

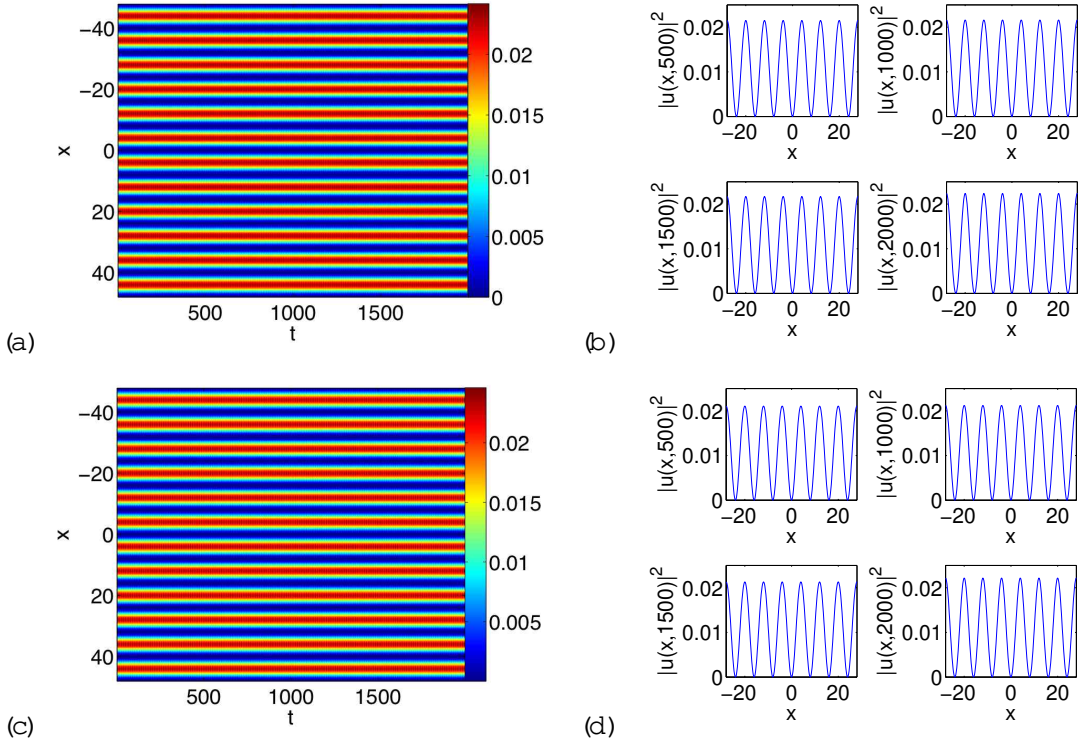


FIG. 6: (Color online) Dynamical evolution of the on-site solutions with $\beta = -2$ for the initial waves of Eq. (23) [panels (a) and (b)] and Eq. (24) [panels (c) and (d)]. In both cases, $V_0 = 0.15$.

observe that the maximum eigenvalue now has a much smaller value and that the ensuing instabilities here are much weaker oscillatory ones. An interesting feature that we note in passing is the formation of "rings" of such oscillatory instabilities (see Fig. 8).

The stability results discussed above can also be considered in light of the recent work [37] on the development of instabilities for NLS equations with constant nonlinearity coefficients and periodic potentials. The authors of Ref. [37] found (among other results) that small-amplitude, periodic, standing-wave solutions corresponding to band edges alternate in their stability, where upper band edges are modulationally unstable in the attractive case and lower band edges are modulationally unstable in the repulsive case. Moreover, the theory in [37] is also applicable to the M AW solutions constructed above, as the resonance relation they satisfy guarantees their spatial periodicity.

To examine the onset of modulation instabilities, we consider small perturbations to the M AWs of the form $u_1 \exp(-i\omega t)$. That is, one linearizes the GP equation (2) around

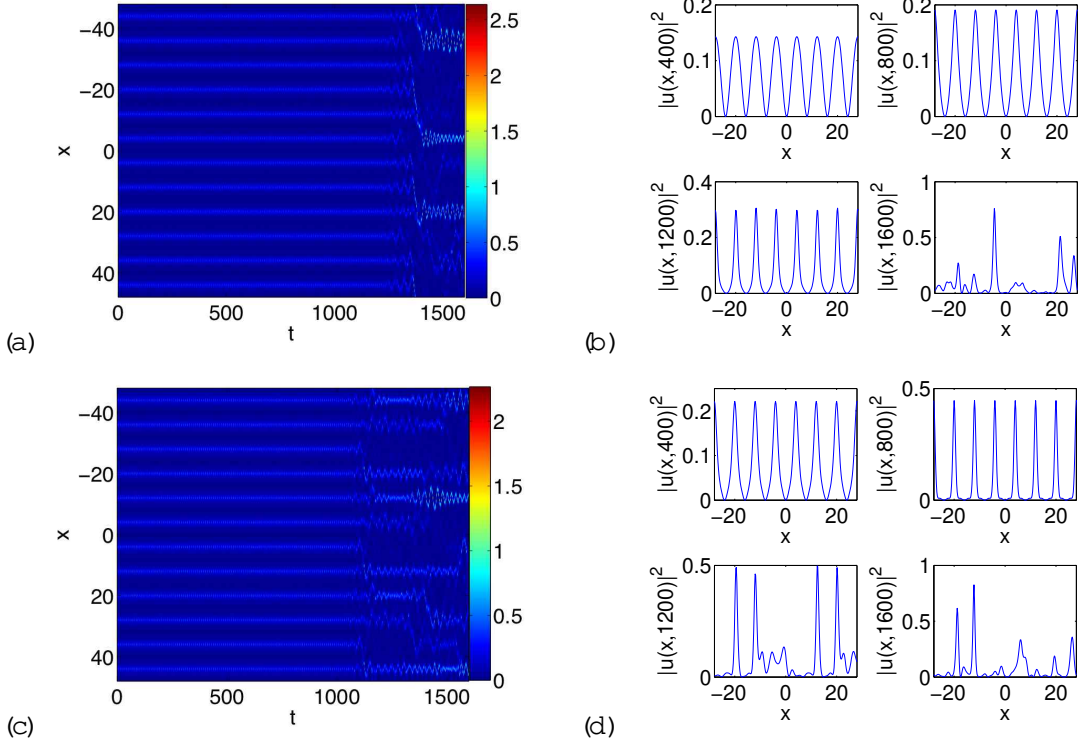


FIG . 7: (Color online) Same as Fig. 6, except for $V_0 = 1.5$. Observe that the solutions now become unstable for times longer than $t = 1000$, highlighting the much weaker nature of the corresponding instability in comparison to its off-site counterpart. The fact that the refined ansatz (24) now seems to become unstable at an earlier time is probably due to the significant change in the profile of the (exact) solution for large V_0 (see Fig. 8).

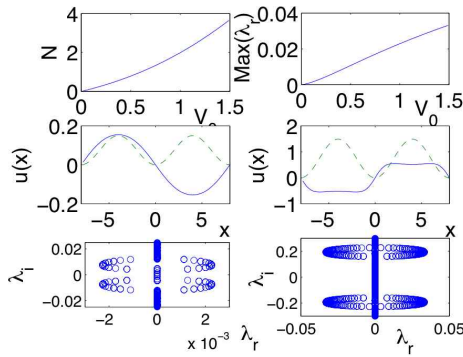


FIG . 8: (Color online) Same as Fig. 5, except for on-site MAWs. In this case, the instability of the solutions is much weaker and is due to a band of oscillatory instabilities.

the M AW solutions.] Such perturbations satisfy the Bogoliubov equations,

$$L_+ p = q; \quad L q = p; \quad (26)$$

where the amplitude $u_1 = p + iq$ and

$$\begin{aligned} L &= \frac{1}{2} \frac{d^2}{dx^2} + V(x) + g(x) j_{\text{M AW}} \frac{d}{dx} & ; \\ L_+ &= \frac{1}{2} \frac{d^2}{dx^2} + V(x) + 3g(x) j_{\text{M AW}} \frac{d}{dx} & : \end{aligned} \quad (27)$$

Recall that in the absence of a linear optical lattice, $V(x) = 0$.

In Ref. [37], it is shown that a sufficient condition for the onset of the modulational instability is for $\lambda = 0$ to be in the interior of a band of the L_+ operator. When $\lambda = 0$, Eqs. (27) decouple, so that $L_+ p = L q = 0$. With the sinusoidal solution (23), we obtain the following Mathieu equations for $V(x) = 0$:

$$\begin{aligned} \frac{1}{2} \frac{d^2 q}{dx^2} + \frac{''c^2}{4} + \frac{''c^2}{4} \cos(2x + 2') q &= 0; \\ \frac{1}{2} \frac{d^2 p}{dx^2} + \frac{3''c^2}{4} + \frac{3''c^2}{4} \cos(2x + 2') p &= 0; \end{aligned} \quad (28)$$

where we recall that $2\sim = 2 + (3=8)''^2 = \lambda^2$, $c = \frac{p}{8} \sqrt{8 - \lambda^2} = 3$, and λ and λ' are free parameters. (Note that the factors of $g(x)$ in (27) cancel out with $g(x)$ factors in $j_{\text{M AW}} \frac{d}{dx}$ because of the transformation used to construct the M AW solutions.) In the Mathieu equation $L_+ p = 0$, the parameter combinations are $3''c^2 = 4 = 2''_1$ and $\lambda^2 = 2 = 3''^2 = 16$. In the limit $''c^2 \rightarrow 0$ (i.e., $V_0 \rightarrow 0$), equations (28) become linear harmonic oscillators.

To examine the applicability of the aforementioned theorem of [37] in the present setting, we have computed the eigenvalues of L_+ . In particular, as a systematic measure for the inclusion of the zero eigenvalue in a band of eigenvalues of L_+ , we consider M in (j_{L_+}, j) , where j_{L_+} denotes the eigenvalues of the operator. We show this diagnostic in Fig. 9 for solutions with $\lambda = 0$. One can see that for $V_0 < 0.5$ (roughly), the 0 eigenvalue is, within the levels of our numerical accuracy, contained in a band of L_+ . This, according to the results of [37], implies the existence of modulational instability in this case. On the other hand, for larger V_0 , this no longer occurs; however, because the criterion only offers a sufficient condition, the results are inconclusive in this latter case. Nevertheless, the full numerical results of Fig. 5 indicate the presence of instability here as well. For $\lambda = 2$, we do not find the 0 eigenvalue remaining in a band of the L_+ eigenvalues for increasing V_0 ; hence, for that case as well, we need to revert to the full numerical results of Fig. 8.

One can also examine the sufficient condition of [37] from a theoretical perspective using properties of Hill's equations. The eigenvalue problem $L_+ p = \lambda_{L_+} p$ is described by the Mathieu equation

$$\frac{d^2 p}{d^2} + [+ 2 \cos(2 + 2)] p = 0; \quad (29)$$

where $\lambda = x$ and

$$= 1 + \frac{2 \lambda_{L_+}}{2} - \frac{4''_1}{8^2}; \quad = \frac{2''_1}{8^2}; \quad (30)$$

From Floquet theory, we construct solutions to (29) of the form $p(\phi) = \exp(-\lambda_{L_+} \phi) Z(\phi)$, where $Z(\phi)$ is a periodic function with period π and λ_{L_+} is known as the characteristic (or Floquet) exponent [38, 39].

Expanding $Z(\phi)$ in a Fourier series and equating each of its coefficients to zero yields an infinite-dimensional matrix, whose determinant $\det(\lambda)$ (the so-called 'Hill determinant') is given by

$$(\lambda) = (0) \frac{\sin^2 \frac{1}{2} i}{\sin^2 \frac{1}{2} p} : \quad (31)$$

The Floquet exponents satisfy $\det(\lambda) = 0$, so they are given by [38, 39]

$$= \frac{2i}{\sin^2(0)} \left(\frac{1}{2} p - \sum_{k=2}^{\infty} \right) : \quad (32)$$

To determine the spectral bands, one then computes the trace of the fundamental matrix of (29), which is given by [40]

$$\text{tr}_M(\lambda_{L_+}) = 2 \cos i(\lambda_{L_+}) : \quad (33)$$

The spectral bands of (29) are defined by the condition $|\text{tr}_M(\lambda_{L_+})| \leq 2$.

Computing $i(0)$ is, in general, nontrivial, but it is permissible to consider a finite-dimensional truncation of the (center of the) Hill matrix provided λ is small. Using the example $\lambda = 0$, the 5×5 -dimensional truncation of the matrix is given by

$$\begin{matrix} & 0 & & & & 1 \\ & 1 & -\frac{1}{16} & 0 & 0 & 0 \\ B & -\frac{1}{4} & 1 & -\frac{1}{4} & 0 & 0 \\ & 0 & -1 & - & 0 & 0 \\ @ & 0 & 0 & -\frac{1}{4} & 1 & -\frac{1}{4} \\ & 0 & 0 & 0 & -\frac{1}{16} & 1 \\ A & & & & & \end{matrix} :$$

With the parameter values $\lambda = -8$, $V_0 = 0.15$, $g = 2$, and $\lambda_1 = 1$ (for which $\lambda = 0.15$), we obtain the plot of $\text{tr}_M(\lambda_{L_+})$ shown in Fig. 10. The eigenvalue $\lambda_{L_+} = 0$ is part of the

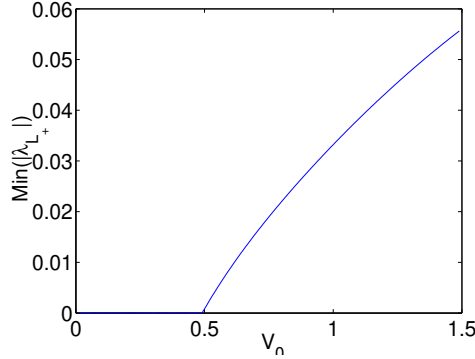


FIG . 9: The eigenvalue of m in minimal magnitude of L_+ as a function of V_0 for $\beta = 0$ solutions. The 0 value of this diagnostic indicates the presence of modulational instability.

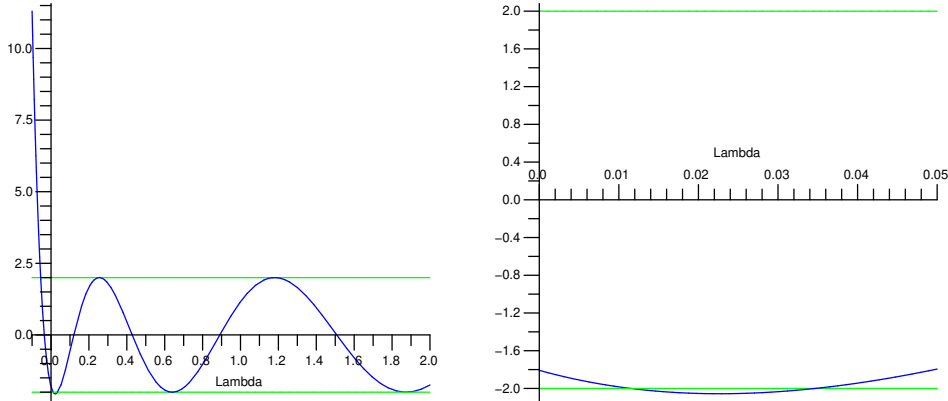


FIG . 10: (Color on line) Trace of the fundamental matrix (vertical axis) versus eigenvalue λ_{L_+} of the L_+ operator. One obtains spectral bands when the magnitude of the trace is bounded by 2. The zero eigenvalue occurs within such a band, indicating that there is a modulational instability. The right panel shows a magnification of the left panel.

band, indicating that a modulational instability occurs. While this semi-analytical approach is presented for completeness and is of interest in its own right, its use of a truncated Hill matrix and of an approximate analytical solution seems to indicate that it is preferable to follow the diagnostic of Fig. 9 presented above.

IV . C O N C L U S I O N S

In this paper, we have investigated the existence and stability of modulated amplitude waves (M AW s) in quasi-one-dimensional Bose-Einstein condensates (BECs) in "nonlinear lattices." In particular, we considered an experimentally feasible situation in which the condensate's s-wave scattering length is modulated periodically in space. We analyzed the relevant Gross-Pitaevskii (GP) equation with a spatially periodic nonlinearity coefficient. We transformed this GP equation into a new GP equation with a constant nonlinearity coefficient and (for small modulations of the scattering length) an effective (quasi-)superlattice potential. We studied spatially extended solutions by applying a coherent-structure ansatz to the latter equation, which leads to a nonlinear generalized Ince equation governing the amplitude's spatial dynamics. In the small-amplitude limit, we used averaging to construct modulated amplitude wave (M AW) solutions, whose stability we examined using both direct numerical simulations of the original GP equation and fixed-point computations used to obtain the M AW s as numerically exact solutions.

While direct simulations suggest stability of the constructed M AW solutions for sufficiently weak periodic modulations, the fixed point computations indicate that even those are weakly unstable (though they can persist long enough to permit experimental observations) for "off-site" solutions, whose maxima do not coincide with maxima of the nonlinear lattice. On the other hand, "on-site" M AW solutions are stable for much longer times even for large periodic modulations of the scattering length. The results are consistent with recent theoretical work in [37] on nonlinear Schrödinger equations with periodic potentials and constant nonlinearity coefficients, suggesting that the theorems therein can be extended to accommodate the collisionally inhomogeneous BECs (such as the spatially periodic scattering lengths examined here).

Acknowledgments: We thank Jared Bronski and Richard Rand for useful comments during the preparation of this paper. M A P . acknowledges support from the Gordon and Betty Moore Foundation through Caltech's Center for the Physics of Information. P G K . acknowledges funding from NSF-DMR-0204585, NSF-CAREER, and NSF-DMR-0505663. B A M . appreciates a partial support from the Israel Science Foundation through the Excellence-Center grant No. 8006/03. D J F . acknowledges partial support from the Special Research Account of the University of Athens.

V . APPENDIX : FUNCTIONS IN THE SECOND-ORDER AVERAGING

In this Appendix, we display some of the functions used in the averaging method in the main text. The generating functions at first order for the resonant case are

$$\begin{aligned} w_1(c;';x) = & \frac{c}{2} \frac{c^2}{4} \cos(2x + 2') + \frac{c}{8} \cos(4x + 2') \\ & + \frac{c^3}{32^2} \cos(4x + 4') - \frac{c}{4} \cos(2x); \end{aligned} \quad (34)$$

$$\begin{aligned} w_2(c;';x) = & \frac{1}{2} \frac{c^2}{2} \sin(2x + 2') - \frac{1}{8} \sin(4x + 2') \\ & - \frac{c^2}{32^2} \sin(4x + 4') - \frac{1}{4} \sin(2x); \end{aligned} \quad (35)$$

The functions L_1 and L_2 that appear at second order are given by

$$\begin{aligned} L_1(c;';x) = & \frac{1}{2} \sin(x + ') \cos(x + ') w_1 D_1 G_1 + \frac{c}{2} \sin^2(x + ') w_2 D_1 G_1 \\ & + \sin^2(x + ') w_1 D_2 G_1 + c \sin(x + ') \cos(x + ') w_2 D_2 G_1 \\ & - \frac{1}{2} \cos(x + ') w_2 G_1 - \frac{1}{2} \sin(x + ') G_2 \end{aligned} \quad (36)$$

$$\begin{aligned} L_2(c;';x) = & \frac{1}{c} \cos^2(x + ') w_1 D_1 G_1 + \frac{1}{c} \cos(x + ') \sin(x + ') w_2 D_1 G_1 \\ & + \frac{1}{c} \cos(x + ') \sin(x + ') w_1 D_2 G_1 + \cos^2(x + ') w_2 D_2 G_1 \\ & + \frac{1}{c} \sin(x + ') w_2 G_1 + \frac{1}{c^2} \cos(x + ') w_1 G_1 - \frac{1}{c} \cos(c + ') G_2; \end{aligned} \quad (37)$$

where $D_1 G_1$ and $D_2 G_1$ denote, respectively, the derivatives of $G_1(s; s^0; x)$ with respect to s and s^0 .

The functions v_1 and v_2 are obtained by integrating the terms in L_1 and L_2 that can be averaged out [i.e., the ones that do not appear in Eq. (25)]. Note that L_2 has seven terms, whereas L_1 has only six. The penultimate term in the former is due to the presence of c in the denominator of the expression for v_0 and arises at second order in the Taylor series because $v_0 = c + "w_1$.

[1] C. Sulem and P.-L. Sulem, *The Nonlinear Schrodinger Equation: Self-Focusing and Wave Collapse* (Springer-Verlag, New York, NY, 1999).

[2] L.Pitaevskii and S.Stringari, *Bose-Einstein Condensation* (Clarendon Press, Oxford, 2003).

[3] Yu.S.Kivshar and G.P.Agrawal, *Optical Solitons: From Fibers to Photonic Crystals* (Academic Press, San Diego, 2003).

[4] R.Folman, P.Kuefer, J.Schmidtmayer, J.Denschlag and C.Henkel, *Adv. Atom. Mol. Opt. Phys.* 48, 263 (2002); J.Reichel, *Appl. Phys. B* 75, 469 (2002); J.Fortagh and C.Zimmermann, *Science* 307 860 (2005).

[5] J.Werner, *Cold and Ultracold Collisions in Quantum Microscopic and Mesoscopic Systems*, Cambridge University Press 2003.

[6] S.Inouye, M.R.Andrews, J.Stenger, H.J.Miesner, D.M.Stamper-Kurn and W.Ketterle, *Nature* 392, 151 (1998); J.Stenger, S.Inouye, M.R.Andrews, H.J.Miesner, D.M.Stamper-Kurn, and W.Ketterle, *Phys. Rev. Lett.* 82, 2422 (1999).

[7] J.L.Roberts, N.R.Claussen, J.P.Burke,Jr., C.H.Greene, E.A.Cornell, and C.E.Williamson, *Phys. Rev. Lett.* 81, 5109 (1998); S.L.Cornish, N.R.Claussen, J.L.Roberts, E.A.Cornell, and C.E.Williamson, *Phys. Rev. Lett.* 85, 1795 (2000).

[8] M.Theis, G.Thalhammer, K.Winkler, M.Hellwig, G.Ru, R.Grimm, and J.H.Denschlag, *Phys. Rev. Lett.* 93, 123001 (2004).

[9] L.You and M.Marinescu, *Phys. Rev. Lett.* 81, 4596 (1998).

[10] M.Olshanii, *Phys. Rev. Lett.* 81, 938 (1998); T.Bergeman, M.G.Moore and M.Olshanii, *Phys. Rev. Lett.* 91, 163201 (2003).

[11] J.Herbig, T.Kraemer, M.Mark, T.Webber, C.Chiu, H.C.Nagerl, and R.Grimm, *Science* 301, 1510 (2003); C.A.Regal, C.Ticknor, J.L.Bohn, and D.S.Jin, *Nature* 424, 47 (2003).

[12] M.Bartenstein, A.Altmeyer, S.Riedl, S.Jochim, C.Chiu, J.Hecker Denschlag, and R.Grimm *Phys. Rev. Lett.* 92, 203201 (2004).

[13] F.Kh.Abdullaev, J.G.Caputo, R.A.Kraenkel, and B.A.Malomed *Phys. Rev. A* 67, 013605 (2003); H.Saito and M.Ueda, *Phys. Rev. Lett.* 90, 040403 (2003); G.D.Montesinos, V.M.Perez-Garcia, and P.J.Torres, *Physica D* 191, 193 (2004).

[14] M.Matuszewski, E.Infeld, B.A.Malomed, and M.Trippenbach, *Phys. Rev. Lett.* 95, 050403 (2005); M.Trippenbach, M.Matuszewski, and B.A.Malomed, *Europhys. Lett.* 70, 8 (2005).

[15] P.G.Kevrekidis, G.Theodoulis, D.J.Frantzeskakis, and B.A.Malomed, *Phys. Rev. Lett.* 90, 230401 (2003); D.E.Pelinovsky, P.G.Kevrekidis, and D.J.Frantzeskakis, *Phys. Rev. Lett.* 91, 240201 (2003); F.Kh.Abdullaev, E.N.Tsoy, B.A.Malomed, and R.A.Kraenkel,

Phys. Rev. A 68, 053606 (2003); F. Kh. Abdullaev, A. M. Kamchatnov, V. V. Konotop, and V. A. Brazhnyi Phys. Rev. Lett. 90, 230402 (2003); Z. Rapti, G. Theodaris, P. G. Kevrekidis, D. J. Frantzeskakis and B. A. Malomed, Phys. Scripta T 107, 27 (2004); D. E. Pelinovsky, P. G. Kevrekidis, D. J. Frantzeskakis, and V. Zhamitsky, Phys. Rev. E 70, 047604 (2004); Z. X. Liang, Z. D. Zhang, and W. M. Liu, Phys. Rev. Lett. 94, 050402 (2005). A. Gubeskys, B. A. Malomed, and I. M. Merhasin, Stud. Appl. Math. 115, 255 (2005); M. A. Porter, M. Chugunova, and D. E. Pelinovsky, e-print [nlin/PS/0507025](http://arxiv.org/abs/nlin/PS/0507025).

[16] F. Kh. Abdullaev and M. Salerno, J. Phys. B 36, 2851 (2003).

[17] H. Xiong, S. Liu, M. Zhan, and W. Zhang, Phys. Rev. Lett. 95, 120401 (2005).

[18] G. Theodaris, P. Schmelcher, P. G. Kevrekidis, and D. J. Frantzeskakis, Phys. Rev. A 72, 033614 (2005).

[19] M. I. Rodas-Verde, H. Michinel, and V. M. Perez-Garcia, Phys. Rev. Lett. 95, 153903 (2005).

[20] A. V. Carpentier, H. Michinel, M. I. Rodas-Verde, and V. M. Perez-Garcia, e-print [cond-mat/0602582](http://arxiv.org/abs/cond-mat/0602582).

[21] G. Theodaris, P. Schmelcher, P. G. Kevrekidis, and D. J. Frantzeskakis, e-print [cond-mat/0509471](http://arxiv.org/abs/cond-mat/0509471);

[22] J. Gamier and F. Kh. Abdullaev, e-print [cond-mat/0605261](http://arxiv.org/abs/cond-mat/0605261).

[23] F. Kh. Abdullaev, and J. Gamier, Phys. Rev. A 72, 061605(R) (2005).

[24] H. Sakaguchi and B. A. Malomed, Phys. Rev. E 73, 026601 (2006).

[25] G. Fibich and X. P. Wang, Physica D 175, 96 (2003).

[26] F. Kh. Abdullaev, A. Gammal, and L. Tomio, J. Phys. B 37, 635 (2004).

[27] S. Peil, J. V. Porto, B. Laburthe Tolra, J. M. Obrecht, B. E. King, M. Subbotin, S. L. Rolston, and W. D. Phillips, Phys. Rev. A 67, 051603 (2003).

[28] V. M. Perez-Garcia, H. Michinel, and H. Herrero, Phys. Rev. A 57, 3837 (1998); Yu. S. Kivshar, T. J. Alexander, and S. K. Turitsyn, Phys. Lett. A 278, 225 (2001); L. Salasnich, A. Parola and L. Reatto, Phys. Rev. A 65, 043614 (2002); Y. B. Band, I. Towers, and B. A. Malomed, Phys. Rev. A 67, 023602 (2003).

[29] M. A. Porter and P. Cvitanovic, Phys. Rev. E 69, 047201 (2004).

[30] M. A. Porter and P. Cvitanovic, Chaos 14, 739 (2004).

[31] M. A. Porter and P. G. Kevrekidis, SIAM J. on Appl. Dynam. Syst. 4, 783 (2005).

[32] M. A. Porter, P. G. Kevrekidis, and B. A. Malomed, Physica D 196, 106 (2004).

- [33] L.Ng and R.Rand, *Nonlinear Dynamics* 31, 73 (2003).
- [34] L.Ng and R.Rand, *Chaos, Solitons and Fractals* 14, 173 (2002).
- [35] B.Deconinck and J.N.Kutz, *J. Comp. Physics*, in press (2006).
- [36] G.Fibich, Y.Sabin, and M.I.Weinstei, *Physica D* 175, 96 (2003).
- [37] J.C.Bronski and Z.Rapti, *Dynamics of PDE* 2, 335 (2005).
- [38] E.L.Ince, *Ordinary Differential Equations* (Dover Publications, Inc., New York, NY, 1956).
- [39] A.H.Nayfeh and D.T.Mook, *Nonlinear Oscillations* (John Wiley & Sons, Inc., New York, NY, 1995).
- [40] D.E.Pelinovsky, A.A.Sukhorukov, and Yu.S.Kivshar, *Phys. Rev. E* 70, 036618 (2004).